Adaptive MPC for a Reefer Container

Kresten K. Sørensen[a], Jakob Stoustrup[b], Thomas Bak[b]

[a]*Lodam electronics, Kævej 77, 6400 Sønderborg, Denmark,*
(email: [kks@lodam.com)
[b]*Department of Automation and Control, Aalborg University, Denmark,*
(email: [jakob, tba]@es.aau.dk)

Abstract

In this work the potential energy saving by adaptation to daily ambient temperature differences for frozen cargo in reefer containers are studied using a model of the Star Cool reefer. The objective is to create a controller that can be implemented on an embedded system and a range of methods are used to reduce the computational load. A combination of MPC and traditional control is used and the accuracy of the MPC is enhanced with an online update of model parameters. Simulation experiments showing potential energy savings of up to 21% where the MPC is allowed to control both the cooling capacity and the ventilation of the cargo are. The largest cost reduction is achieved through a reduced ventilation rate.

Keywords: Adaptive Control, MPC, Refrigeration, Parameter Estimation, Set-Point Optimization, Reefer Container.

Nomenclature

Latin symbols

M	Mass (kg)
Q	Energy flow (W)
V	Volume (m^3)
T	Temperature (C°)
c	Specific heat (J/(Kg K))
UA	Heat transfer coefficient (W/K)

Subscripts

air	Air in the cargo hold
amb	Ambient
floor	Floor of the cargo hold
cool	Cooling capacity
fan	Evaporator fan
cargo	Cargo inside the cargo hold
sup	Supply air to cargo hold
ret	Return air from cargo hold
box	Walls of the cargo hold

1. Introduction

Today a large amount of perishable cargo is transported by sea in reefer containers. By mid-2008 the fleet consisted of 4500 reefer-vessels with a combined reefer capacity of 11.4 million TEU[1] and the capacity is predicted to grow by 69% by 2013, see [1]. The reefer containers are powered by electricity with a consumption of up to 6kW per TEU, depending on the ambient temperature and the temperature inside the container itself. With an average consumption of 3.6kW per TEU this yields a combined consumption 41GW which is, on average, 8.9MW per ship; see [2] and [3]. Previously this was seen to be insignificant with respect to the large amount of energy used to propel the ship, but due to rising oil prices, harder competition in the shipping market and the environmental impact of shipping it has become interesting to reduce the energy consumption of reefer containers.

The control solutions currently employed are based on classical control theory where the individual components are controlled by separate controllers, with a limited amount of controller interconnections and gain scheduling. The objective of these controllers is to keep the temperature inside the container close to a set point at ambient temperatures between -20C$^\circ$ and +37C$^\circ$ (hot side). The set point is in the range of -29C$^\circ$ and +25C$^\circ$ (cold side). Due to the large range of operation on the hot and cold side and the non-linearities in the refrigeration system the controllers used must be conservative in order to give stability over the entire area of operation.

Fruit and vegetables are usually quite sensitive to variations in temperature and atmosphere and this means that the cargo temperature and air composition in the container must be kept within certain limits. This reduces the potential for control optimizations with respect to energy consumption by using the thermal inertia of the cargo as a buffer. It has been shown that the cost of operating a refrigeration system may be lowered by using thermal inertias in the system as a buffer to offset cooling to periods where the cost is low. In [4] the cost of a running household heat pump is lowered, using an MPC that is fed the forecasted cost of electricity. Exploitation of ambient conditions to lower the energy consumption of building HVAC systems, while respecting occupant comfort constraints are demonstrated in [5, 6, 7, 8], and shown to significantly reduce energy consumption while ensuring good occupant comfort. A learning based approach to pre-cooling of foodstuffs to avoid saturation of the refrigeration system on hot days are demonstrated

[1] Twenty Foot Equivalent. The equivalent of a twenty foot reefer container.

by [9], using an MPC that is updated online with the learning based constraints and predicted future load. In [10] MPC is used to control the product quality of chilled cargo in refrigerated containers with the main focus on modeling and control of the cargo quality, resulting in a reduction of mass loss in the cargo due to evaporation and lower energy consumption due to reduced ventilation rate.

An existing energy saving control strategy in use is QUEST, see [11], which is a control scheme for fruit and vegetables that allows for bigger supply air temperature variances and lower fan speeds, based on a predefined set of rules. This can be allowed because research has shown that there is no degradation of produce quality if the supply air temperature is varied around the set-point due to the thermal insulation of the produce packaging and the slow metabolic rates of the produce, see [12]. The rules for ventilation rate and temperature variation have been found by testing a wide range of different types of fruit and vegetables and ensuring that cargo quality remains unaffected by the variations. There are different rules for different product classes and they have been designed dependent of the temperature set-point in order to make it easy to operate. This is important because it is infeasible to educate loading crews all over the world in complex set up procedures. For reefer containers without a VSD (Variable Speed Drive) on the compressor, the energy savings from using QUEST can be as much as 53% due to the fact that the refrigeration system is very inefficient at part load and for containers with a VSD on the compressor the savings are smaller but still significant.

For frozen goods, the rules that must be observed in order to preserve cargo quality are more lenient than for chilled goods, and therefore the cargo thermal inertia can be used to offset cooling from the periods where the system is less efficient to periods where the system is more efficient. The ambient temperature has a direct influence on the condensation pressure and thereby also the system efficiency which leads to the possibility of moving some cooling from the day where the ambient temperature is high to the night where the ambient temperature is lower. Another way of reducing energy consumption is to reduce the amount of ventilation inside the cargo hold because the power consumed by the fans has a double impact on the cost of running the system. The fans consume energy that is added to the cost of running the system but the kinetic energy the air receives from the fans is eventually converted to heat inside the container which means that it must be removed by the refrigeration system. Therefore it could be interesting to investigate the potential in an optimization of how the fans are used.

Model Predictive Control (MPC) was introduced in the petro-chemical industry in order to control difficult processes with long delays and unknown states but

today it is used in a wide range of applications such as power plant control and the automotive industry. MPC is used for optimizing control of processes with respect to known future demands or known future changes in external conditions, while keeping within a given set of constraints. The performance of MPC is dependent on the quality of the model on which it is based because it is used to predict the behavior of the system over the prediction horizon. For systems where the model dynamics may change either a non-linear or adaptive linear approach must be used in order to keep performance and avoid violating constraints.

A refrigeration system has several degrees of freedom, meaning that the same cooling capacity can be obtained with different actuator set-points. It was shown by [13] that selecting the correct set-points can have a high impact on the efficiency of the refrigeration system and therefore any controller aiming to save energy should observe this.

In this study the potential for energy saving by adaptation to daily ambient temperature differences is studied for frozen cargo in refrigerated containers. The observation that adequate cooling may be achieved at a lower ventilation rate that was done in [10] is used to formulate control laws for an MPC that ensures optimal utilization of the fans when they are running. Cargo parameters such as thermal inertia and heat transfer coefficient are estimated and used as basis for the MPC model, resulting in flexibility towards changes in these parameters that does not exist in QUEST. Furthermore the MPC is set up to exploit daily variations in ambient temperature by cooling more when the ambient temperature is low and the efficiency of the refrigeration system is higher. This extra cooling is ”stored” in the cargo thermal inertia allowing for a smaller cooling effort during the day when the ambient temperature is high and the refrigeration system efficiency is low. The future ambient temperature is predicted from measurements from the last 24 hours by an oscillator and a simple phase-locked loop and fed to the MPC.

In this paper we present an adaptive MPC controller that utilizes the same principles as QUEST but with the added benefit of adaptation to cargo parameters and daily cycles in ambient temperature for increased energy efficiency. The potential energy savings at different ambient temperatures and fan control methods are investigated and presented. The computational load is reduced due to different step sizes in the prediction horizon and linearizing local controllers enabling the use of a reduced linear model for the MPC.

In the following the methods used in this paper is described, starting with a short introduction to the refrigeration system in Section 2.1. Then follows a description of the parameter and state estimators used by the controller in Section 2.2 and finally the controller itself is described in Section 2.3.

2. Methods

2.1. Refrigeration System Simulation Model

The refrigeration container used in this paper is built by *Maersk Container Industry* and equipped with a *Star Cool* refrigeration unit, see [14]. A Refrigeration container is an insulated box with a door for cargo loading in one end and a refrigeration system in the other, as shown in Figure 1.

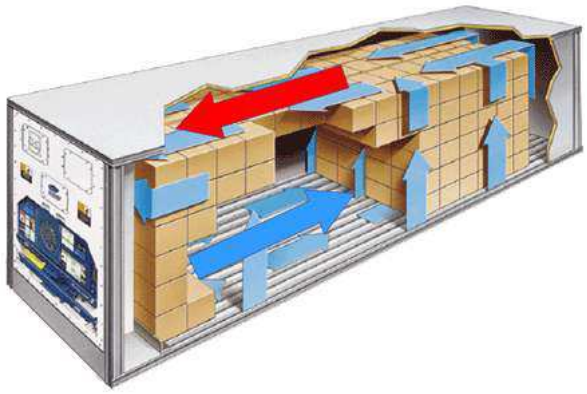

Figure 1: Airflow in the Refrigeration Container

The cargo is kept cold by air that is circulated from the evaporator and towards the back of the container through a T-profile floor that allows air to enter small gaps between the produce. The air is heated by the produce or the walls and rises to the ceiling of the box where the hot air flows back to the evaporator. Natural convection is not enough to ensure an even distribution of air in the box and therefore the air flow is driven by fans located above the evaporator. The energy from these fans ends up as heat in the box and has to be removed by the refrigeration system. Therefore it is desirable to run the fans as little as possible. It is however necessary to start the fans at regular intervals in order to be able to measure the air temperature in the box itself because no air temperature sensors is placed here, and in order to avoid local hot-pockets of air to build up and spoil the produce.

The schematic of the refrigeration system used in this study is shown in Figure 2. It is a two-stage cycle, using an economizer to increase the efficiency of the system at high temperature differences between the cold and hot side.

The compressor has a high- and low pressure stage shown as two single-stage compressors in the figure. The compressor is equipped with a VSD and the fans

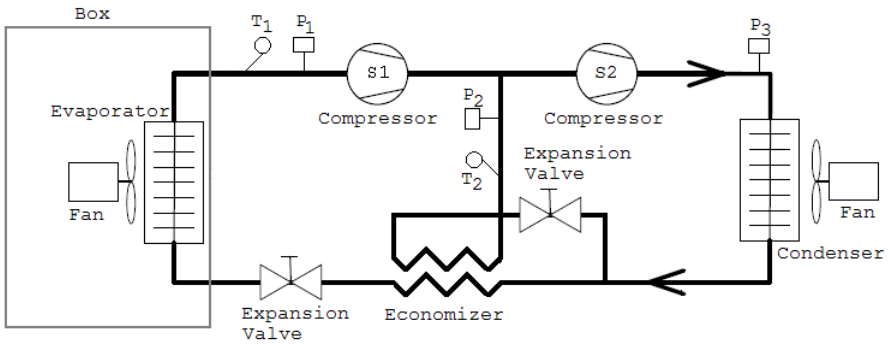

Figure 2: Refrigeration System Schematic

may be either stopped, at half speed or at full speed. The expansion valves are pulse modulated, that is they can either closed or fully open, and therefore they are controlled by a PWM signal with a period of six seconds.

The reefer container has been modelled in detail and a simulation model that accurately reflects the refrigeration system and cargo dynamics at a one second resolution, is available. The comparison of the different controllers must be done under comparable ambient conditions in order to minimize the uncertainties on the results and therefore the simulation model is used. It has 81 states and models the flow, energy and mass of the refrigerant of the components shown in the system schematic in Figure 2. The simulation model has been verified against a refrigerated container packed with 20,000kg of pork meat and the results of the verification can be seen in Figure 3. The verification consists of a the simulation model running in open loop for three hours using control inputs that was recorded from a real container during a series of capacity steps. The output of the model on the variables significant for control is then compared to the recorded measurements of the same variables from the real system. Figure 4 shows the error distribution of the test from which it can be seen that the model is a good match to the real system. The model verification is carried out at the same temperature set point as the controller in this study is tested at.

2.2. Parameter and State Estimation

Model predictive control requires an accurate model of the system that is to be controlled and a prediction of the trajectory of external conditions relevant the objective of the controller. In this subsection the methods that were used to predict future ambient temperature and estimate the temperature, heat transfer coefficient and heat capacity of the cargo are described.

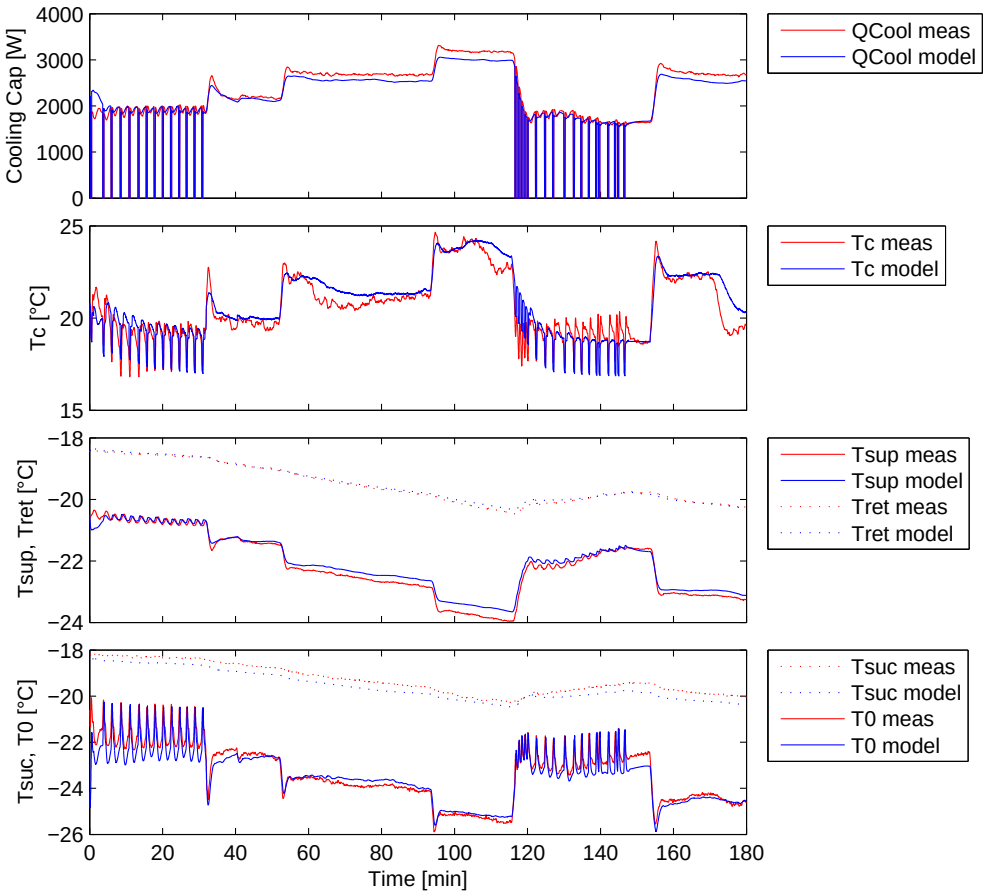

Figure 3: Simulation model verification results

2.2.1. Ambient Temperature Prediction

The ambient temperature must be predicted 24 hours into the future as a reference to the MPC in order to be able to exploit its daily cycles and an observer is constructed for this. Because the temperature is an oscillation with a period of 24 hours an oscillator is used and synchronized by a Phase Locked Loop (PLL). For simplicity the prediction is only based on measurements from the past 24 hours, even if more data is available. In Figure 5 the predictions for the first 100 hours of a container's journey from a Danish port are shown, with five hours between each of the predictions.

It can be seen that for the first 24 hours where the measurement set is incomplete the prediction is unreliable, but after that the PLL is locked and the prediction

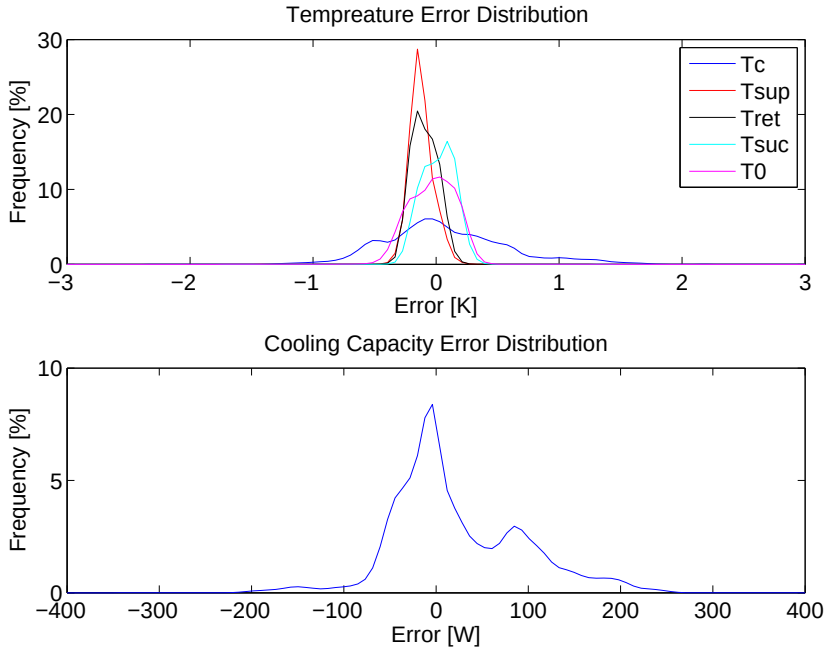

Figure 4: Simulation model error distribution

gets better. Due to a non-sinusoidal oscillation of the measured ambient temperature the amplitude estimate can be off but as shown later the most important thing is that the phase is right and therefore this predictor is adequate for the MPC.

2.2.2. Cargo State and Parameter Estimation

The quality of the solution to the optimization problem in the MPC is dependent on the accuracy of the linear model used. While the properties of the refrigeration system are well defined the properties of the cargo are very uncertain because reefer containers are used to transport a wide range of different goods. The largest thermal mass is usually the cargo and therefore also the most interesting property with respect to exploitation of daily variances in ambient temperature. If the cargo heat capacity is not known the lowest value must be used, in order to ensure that the constraints are not violated, because the lowest heat capacity also gives the fastest dynamics. Using the lowest possible heat capacity will limit the degree to which the variations in COP can be exploited. To resolve this issue a combined parameter estimator and unknown input observer is introduced and the estimates are then used to update the MPC online. The observer is based on the model of the reefer containers cargo hold and cargo that is present in the simula-

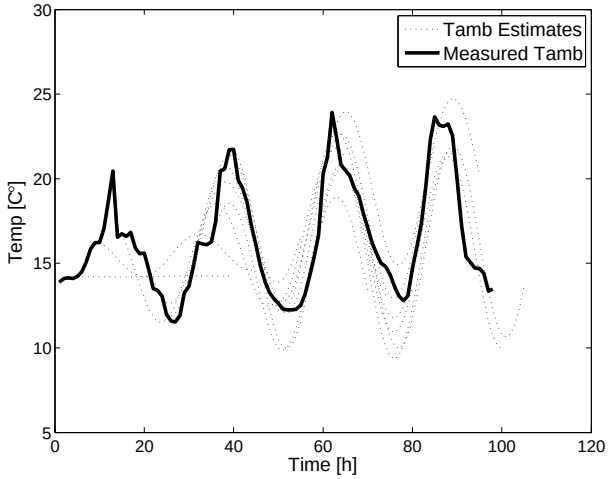

Figure 5: Prediction of future ambient temperature

tion model described in Section 2.1. It has been modified to simulate the unknown states and estimate and update the parameters for the cargo when conditions allow. Knowledge of parameter and state constraints are incorporated and used to ignore corrections that are outliers and select sensible start conditions.

The unknown states and parameters that must be estimated are shown in the following table:

Description	Unit
Cargo heat capacity, C_{cargo}	J/K
Cargo heat transfer coefficient, α_{cargo}	W/K
Cargo temperature, T_{cargo}	°C
Aluminum T-floor temperature, T_{floor}	°C

The heat capacity is the amount of energy required to elevate the cargo temperature one Kelvin and the total heat transfer is the surface area of the cargo multiplied with the heat transfer coefficient. The estimation has to be done online and must be based on the available measurements and actuator signals which are the air return temperature T_{ret}, the air supply temperature T_{sup}, the ambient temperature T_{amb} and the fan speed V_{fan}.

The state equations for the model of the cargo and cargo hold are given by

Equations (1) to (3)

$$\dot{T}_{air} = \frac{Q_{Cargo\rightarrow air} + Q_{amb\rightarrow air} + Q_{fan} + Q_{floor\rightarrow air} - Q_{cool}}{M_{air} \cdot Cp_{air}} \quad (1)$$

$$\dot{T}_{cargo} = \frac{-Q_{cargo\rightarrow air}}{C_{cargo}} \quad (2)$$

$$\dot{T}_{floor} = \frac{Q_{amb\rightarrow floor} - Q_{floor\rightarrow air}}{M_{floor} \cdot Cp_{floor}} \quad (3)$$

The change in air temperature is given by Equation (1) as the sum of all energy flows going to the control volume divided by the heat capacity of the air. This equation is essential for the estimator because the amount of energy going from the cargo to the air, Q_{cargo}, can be derived from it. The average of the measured supply temperature T_{sup} and return air temperature T_{ret} is assumed to be equal to T_{air}. In Equation (2) the change of the unknown state T_{cargo} is given as the energy going from the cargo to the air divided by the estimated heat capacity of the cargo. The last of the state equations (3) gives the change in temperature in the aluminum floor of the container and this has been included in the model because it has a very strong thermal coupling to the air end therefore also significantly slows down the dynamics of the air temperature. The heat transfers in the above equations are given by Equations (4) to (7):

$$Q_{amb\rightarrow air} = (T_{amb} - T_{air}) \cdot 0.810 \cdot \alpha_{box} \quad (4)$$

$$Q_{amb\rightarrow floor} = \left(T_{amb} - T_{floor}\right) \cdot 0.190 \cdot \alpha_{box} \quad (5)$$

$$Q_{floor\rightarrow air} = \left(T_{floor} - T_{air}\right) \cdot \alpha_{floor} \quad (6)$$

$$Q_{cargo\rightarrow air} = (T_{cargo} - T_{air}) \cdot \alpha_{cargo} \quad (7)$$

$$Q_{cool} = f\left(T_{sup}, T_{ret}, V_{fan}\right) \quad (8)$$

$Q_{amb\rightarrow air}$ is the heat transfer from the surroundings to the air in the container through the walls, roof and ends of the cargo hold given by the temperature difference multiplied with the heat transfer coefficient α_{box} and the fraction of total surface area represented by the walls, roof and ends. The floor of the container is also receiving some heat from the outside, given by Equation (5) as the temperature difference multiplied with the heat transfer coefficient α_{box} and the fraction of total surface area represented by the floor. The heat transfer from the floor to the air is given by Equation (6) where the heat transfer coefficient α_{floor} has been found by simple step response experiments. The energy going from the cargo to the air, $Q_{cargo\rightarrow air}$, is given by equation (7) and it includes two unknowns; the

cargo temperature T_{cargo} and the heat transfer coefficient from cargo to air α_{cargo}. T_{air} is the mean of the supply and return temperature for the air entering and leaving the cargo hold which is measured and therefore very reliable.

There is an uncertainty on the heat influx through the container wall depending on the air flow over the outside surface, rain and direct exposure to the sun. From (1) it can be seen that this will give an uncertainty on the estimation of $Q_{cargo \rightarrow air}$ because Q_{fan}, $Q_{floor \rightarrow air}$ and Q_{ref} are known or can be measured.

The easiest state to estimate is the floor temperature because it will reach steady state equilibrium between the ambient and air temperatures which are both measured and therefore if the floor temperature is estimated using equations (5), (6) and (3) the estimated floor temperature will over time track the actual floor temperature.

The cargo temperature may be estimated using the same method as for the floor because it converges towards the air temperature, but this estimate includes the uncertainty of the parameters α_{cargo} and C_{cargo}. If Equation (7) is inserted into Equation (2) and rearranged

$$\dot{T}_{cargo} = (T_{cargo} - T_{air}) \cdot \frac{\alpha_{cargo}}{C_{cargo}} \tag{9}$$

it is clear that the change in cargo temperature is a first order filter on the temperature difference between the air and the cargo, with a time constant that is given by the two unknown parameters. Therefore the cargo temperature estimate will converge towards the mean air temperature, but only be accurate if the estimates of α_{cargo} and C_{cargo} are accurate as well.

A controller that use the thermal inertia of the cargo to offset cooling to more efficient conditions will cool the cargo in pulses that in this case have a duration of several hours, where the cargo is decreased towards the lower temperature constraint. This excitation of the cargo dynamics is exploited to estimate the two unknown cargo parameters α_{cargo} and C_{cargo}.

It is assumed that the system is linear and time invariant (LTI) and therefore it can be assumed that the heat transfer constant and the heat capacity of the cargo are constant over time. This can be used to estimate α_{cargo} by combining Equation (7) and Equation (10) and setting up two equations with two unknowns that is solved for α_{cargo}.

$$
\begin{aligned}
Q_{cargo\rightarrow air-calc} &= Q_{cool} - Q_{amb\rightarrow air} - Q_{floor\rightarrow air} - Q_{fan} && (10)\\
Q_{cargo\rightarrow air-calc-t1} &= \left(T_{cargo-t1} - T_{air-t1}\right)\cdot \alpha_{cargo} && (11)\\
Q_{cargo\rightarrow air-calc-t2} &= \left(T_{cargo-t1} + T_{cargo-delta} - T_{air-t2}\right)\cdot \alpha_{cargo} && (12)\\
\alpha_{cargo} &= \frac{Q_{cargo\rightarrow air-calc-t2} - Q_{cargo\rightarrow air-calc-t1}}{T_{air-t1} - T_{air-t2} + T_{cargo-delta}} && (13)
\end{aligned}
$$

The measurements $Q_{cargo\rightarrow air-calc}$, T_{cargo} and T_{air} in Equations (11) and (12) must be taken at two different times that have a significant difference in $Q_{cargo\rightarrow air-calc}$, in order to produce a reliable estimate of α_{cargo}. $T_{cargo-delta}$ is the estimated change in cargo temperature between the two sample points and because the cargo dynamics are significantly slower than the dynamics of the air, this change can be obtained from the estimated cargo temperature given by Equation (2). In order to prevent inaccurate estimates due to disturbances from the controller it is required that the slope of T_{sup} is smaller than $0.01K/s$ before the first set of measurements are acquired, because this means that cooling capacity is stable. After 15 minutes the second set of measurements are acquired and if the energy flows to the cargo differs by more than 100W and update of α_{cargo} is performed. The maximum allowed change of the estimated heat transfer coefficient is $\pm 50\frac{J}{kg\cdot K}$ for each update.

The heat capacity of the cargo are more difficult to estimate because the estimate has to be inferred from the rate of change in air temperature measurements, and the rate of change in the calculated energy flow from the cargo to the air. At a temperature set-point of -20°C the refrigeration system is able to cool the cargo with up to 4kW which over a period of one hour is enough to cool the cargo used in this study by 0.686K. This means that the slopes involved are very small, and the result is sensitive to noise and disturbances. As for α_{cargo} this may be resolved by determine the slopes over a period of time, and thereby reduce the impact from noise and disturbances.

The slope of the difference between the cargo temperature and the mean air temperature is given by Equation (14)

$$
\begin{aligned}
\dot{T}_{cargo\rightarrow air-diff} &= \dot{Q}_{cargo\rightarrow air-calc}\cdot \alpha_{cargo} && (14)\\
\dot{T}_{cargo} &= \dot{T}_{cargo\rightarrow air-diff} + \dot{T}_{air-mean} && (15)\\
C_{cargo} &= \frac{Q_{cargo\rightarrow air-calc}}{\dot{T}_{cargo}} && (16)
\end{aligned}
$$

and the derivative of cargo temperature can therefore be calculated as in Equation (15). In order to acquire accurate derivatives the period of acquisition should be as long as possible. The estimator requires an hour where the cooling capacity of the refrigeration system is constant and large enough to ensure that at least 1kW of cooling is applied to the cargo, before an update of the heat capacity of the cargo is calculated as shown in Equation (16). On Figure 6 the result of running the estimator on data from a real reefer container packed with 20,000kg of bacon can be seen. On the top axes the supply and return air temperatures are shown

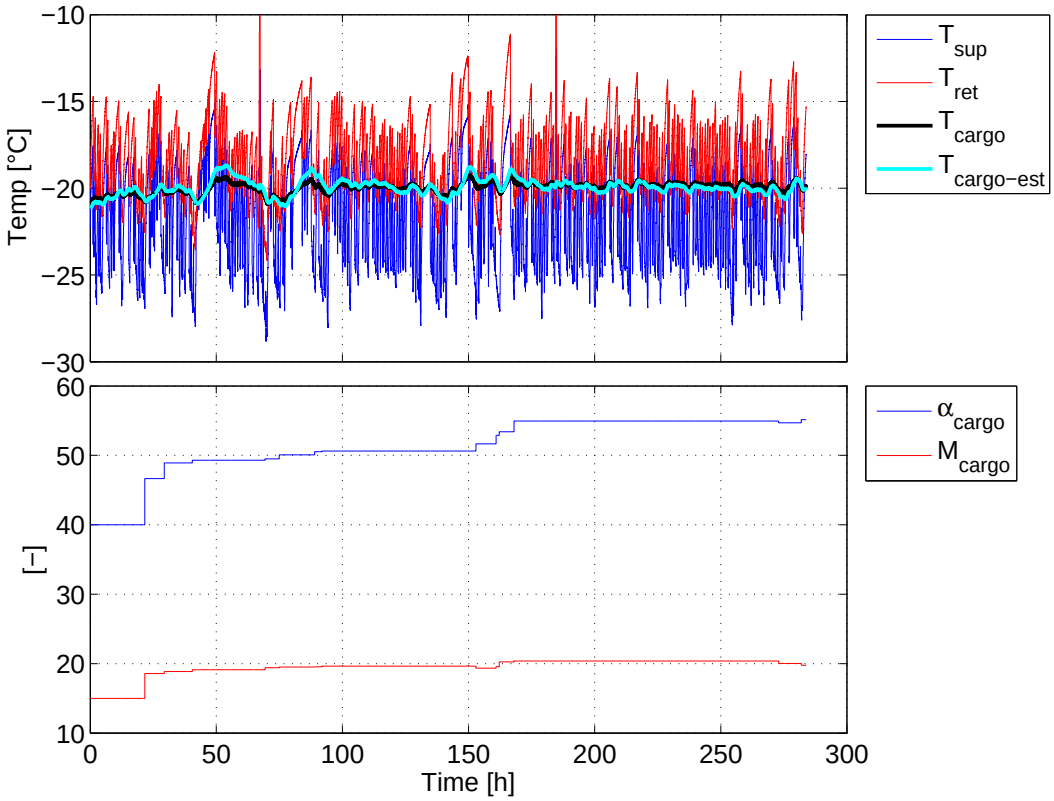

Figure 6: Cargo parameter estimator on reefer container measurements

together with the measured and estimated cargo temperature. The estimated heat capacity of the cargo has been converted to mass in metric tons, using the specific heat capacity for bacon which is $1050\frac{J}{kg \cdot K}$ [15], and should therefore level out around 20. The estimated heat transfer coefficient of the cargo has been divided by 10 in order to better show the details of the results. The data was obtained from a reefer that was located in an open field and therefore subject to the disturbances

from the weather.

The controller was an early attempt at offsetting some cooling from day to night using MPC, but without the estimator for the cargo parameters. The cooling that is applied, is mainly in pulses of 10 minutes which unfortunately is a poor basis for estimating the cargo heat capacity, because the pulses are too short to reliably estimate the change in cargo temperature through the air temperature. Therefore the estimate of the cargo heat capacity is update only 15 times. The heat transfer coefficient for this cargo has been estimated to be 550W/K from the measured cargo and air temperature and the calculated power to the cargo.

On Figure 7 the result of the parameter estimation algorithm running on results from the simulation model with an α_{cargo} of $550\frac{W}{K}$ and a 20,000kg cargo mass with a specific heat capacity of $1050\frac{J}{kg \cdot K}$ is shown. Measurement noise has

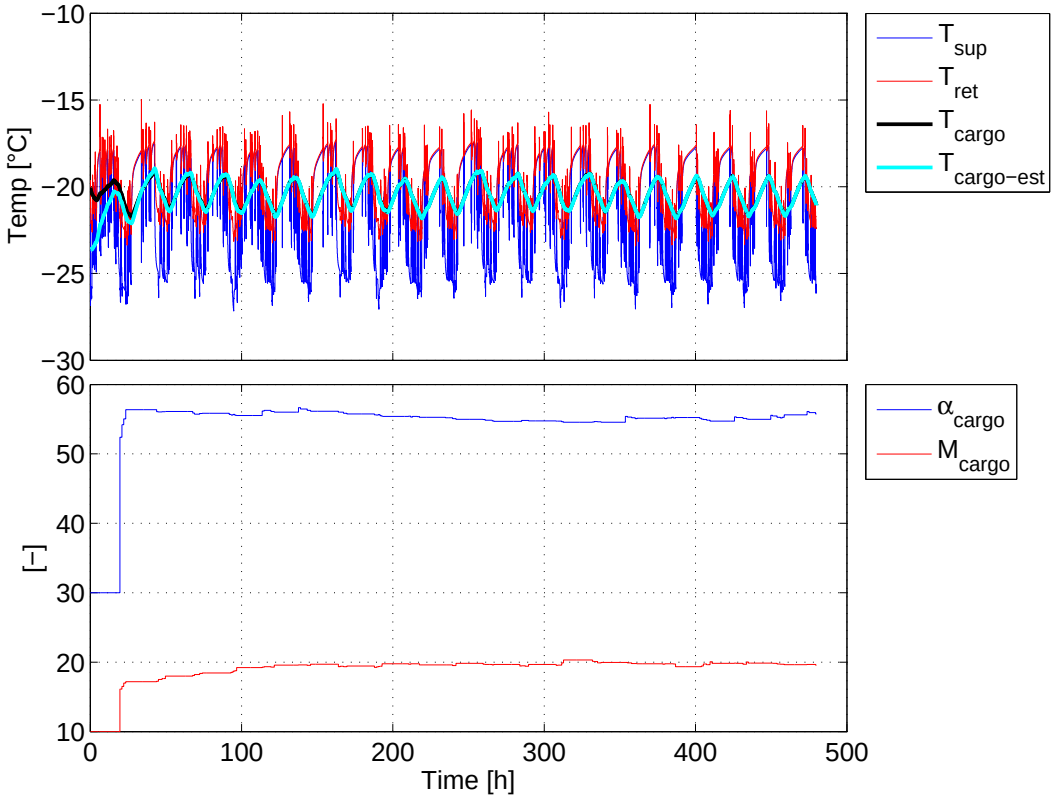

Figure 7: Cargo parameter estimator on simulation model

been added to the simulation results and the values of α_{cargo} and M_{cargo} have been scaled by 10 and 1000 respectively for easier plotting. It is expected that α_{cargo}

converge towards 55 and that M_{cargo} converge towards 20. The estimates quickly converge towards the true values right after start up and within 24 hours the estimates are accurate. In this test the start values have been set to demonstrate convergence but it is often possible to deduce the type of cargo from the temperature set-point and from that select better start values which will enable faster estimator convergence.

2.3. Controller Setup

A non-linear simulation model has been developed as described in Section 2.1 but this model has 81 states and a reduced model is desired, because the controller eventually is to be used on an embedded hardware platform with limited resources. The objective of this study is to exploit the daily cycles in ambient temperature and COP. In order to exploit daily variations in ambient temperature the MPC prediction horizon must be at least 24 hours and if it is to control the fast dynamics directly the resolution must be high. This leads to a high computational load due to the many steps in the prediction horizon and an alternative must be found. A large part of the simulation model dynamics are much faster than the ones relevant to the long term objective and therefore a reduced model containing only the slow states is derived for the MPC. The proposed set up is shown on Figure 8.

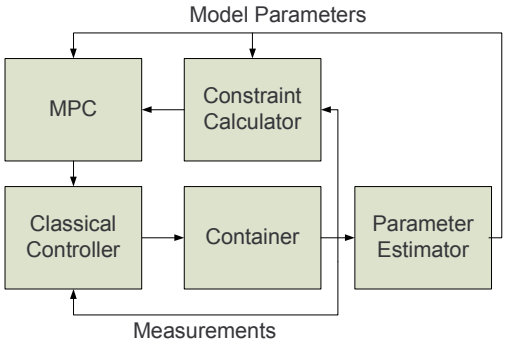

Figure 8: Overall Controller Block Diagram

Because the MPC only handles the slow dynamics a classical controller is inserted between the MPC and the plant (container) in order to do closed loop control of the fast dynamics, while accepting set points from the MPC, see [16, 17]. This has several benefits; Firstly the model for the MPC can be heavily reduced because only the states directly relevant to the objective are needed. Secondly the resolution of the prediction horizon can be reduced because the model for the MPC only has slow dynamics. Thirdly it is possible to use linear MPC because of

the linearizing effect of the classical controller. This is of course only obtainable if the interface between the MPC and the classical controller can be chosen such that the level of abstraction created by the classical controller is high enough to mask the non-linear dynamics while still being able to effectively control all the inputs relevant to the MPC objective.

2.3.1. Interface from MPC to Linearizing Controller

According to [18] the dominant dynamics of a refrigeration system are the thermal constants of the metal surfaces in the heat exchangers and the refrigerant mass time constants, with respect to control applications. The largest thermal mass in the refrigeration system itself is the evaporator that has a mass of 23kg yielding a heat capacity of 20.7 kJ/K but the T-floor has a heat capacity of 2.7 MJ/K and a typical cargo of frozen meat has a heat capacity of 100 MJ/K. This gives a separation of dynamical speed that is several orders of magnitude, between the cargo and the refrigeration system but the temperature of the air is problematic. The heat capacity of the air in the box at -20 C$^\circ$ is 95.36 kJ/K and this is not far from that of the evaporator but because of the thermal coupling to the T-floor and cargo the actual dynamics of the air temperature are much slower. The important factor is the response from the supply temperature T_{sup} to the return temperature T_{ret} and since the air has to flow over both the T-floor and the cargo, the response is slowed considerably. The T-floor alone is enough to leave a comfortable gap in dynamical speeds between the dynamics that must be controlled by the MPC and the nonlinear refrigeration system dynamics.

It is chosen that the reference from the MPC to the classical controller shall be the cooling capacity Q_{ref}, because it has a direct and nearly linear effect on the cargo temperature. The proposed controller set up is shown on Figure 9.

The cooling capacity reference from the MPC is discrete, that is, it changes instantly and stays constant until the next update from the MPC. It is infeasible for the refrigeration system to follow such a reference and therefore an integrator on the difference between actual and requested cooling capacity is added to remove the error from lag in the refrigeration system.

2.3.2. Linearizing Controller

The linearizing controller is a non-linear feed forward, that is based on the model, with a traditional PI controller to correct for inaccuracies and this ensures that the system reaches the capacity requested by the MPC quickly. The actuators controlled by this controller are the condenser fan, the compressor and the expansion valves for the evaporator and the economizer. The compressor has a

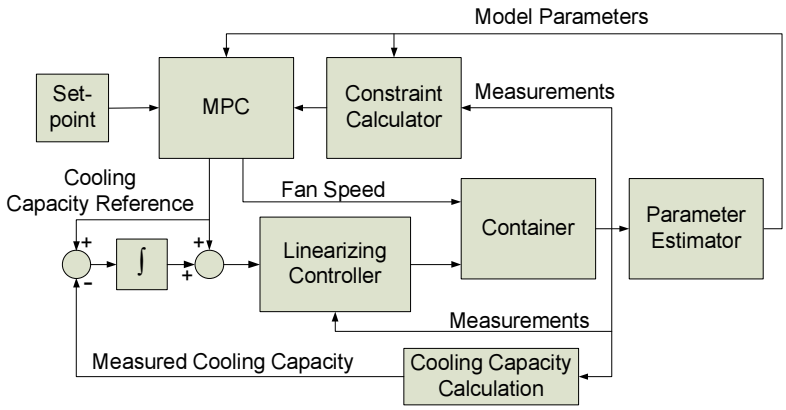

Figure 9: Controller Block Diagram

minimum on time of 30s that must be observed and therefore the rules for this is also built into the linearizing controller. The linearizing controller was tested on the reefer container packed with bacon that is the basis of this study. The test results can be seen on Figure 3, where the reefer is taken through a series of cooling capacity request steps that the reefer must then follow.

2.3.3. Model Predictive Controller

The MPC is constructed using Yalmip, see [19], with the objective of reducing the amount of energy consumed by exploiting daily variations in temperature and therefore the prediction horizon should be at least 24 hours. The maximum step size is limited by the fastest dynamics that must be controlled, in this case the air temperature. A step size of ten minutes is required in order to have adequate control of the air temperature, but this leads to a prediction horizon of 144 steps which is estimated to be too computationally heavy for the embedded hardware. It is therefore chosen to solve this problem by dividing the prediction horizon, see [20], in two sections with different step sizes; at first one with six ten-minute steps and after those 23 steps of one hour each, as shown in Figure 10.

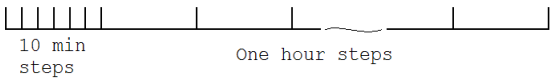

Figure 10: Prediction Horizon

The MPC runs once an hour and the first six ten-minute steps are then implemented one by one after which the process starts over again and the advantage of

this approach is that fine-grained control can be achieved while the total number of steps and iteration frequency remains low. For this system fine grained control is an advantage because the most efficient point of operation in some instances delivers more cooling than needed to keep the temperature and therefore the best option is to run at the optimal cooling capacity for shorter time and by dividing the first hour into six smaller steps, the effective minimum capacity that can be delivered per hour is reduced to a level that is more suitable for this application.

2.3.4. Cost Calculation and Constraint Setup

The evaporator fan circulates the air that moves energy from the box to the evaporator and therefore it is required to run while the compressor is turned on. The power consumption of the fan has an impact on the cost of running the system in two ways; There is the direct power driving the fan and the heat generated by the fan that must be removed again, by the refrigeration system. Because the fan speed is controlled in discrete steps it is important to model this behavior in the actuator constraints of the controller. This is done by declaring the fan speed as a binary variable, which transforms the problem to a mixed integer program. The resulting constraint is shown in Equation (19).

The fan speed variable M_{fan} is 1 when the fan is turned on and Q_{min} and Q_{max} are the constraints on the cooling capacity, calculated on basis of the current operating point. From the above equation it is obvious that Q_{cool} is required to be zero when the fan is turned of and it is constrained by Q_{min} and Q_{max} when the fan is turned on.

The maximal cooling capacity of the refrigeration system is dependent on suction pressure and thereby the temperature in the box and therefore Q_{max} and Q_{min} from Equation 19 must be calculated from the box temperature. This is done from manufacturer data given as polynomials according to [21].

In many real systems we encounter a nonlinear cost on a control input, typically due to decreasing efficiency as the speed of an actuator increases. This is also the case for this system but only to a limited degree for the compressor. The biggest change in COP for the refrigeration system is dependent on the ambient temperature because it has a strong coupling to the discharge pressure that is a determining factor on the amount of work done by the compressor. In Figure 11 the COP of the system is shown for a fixed set point of -20°C and varying cooling capacity and ambient temperature is shown.

The dotted line is the COP of the system when the compressor is running in PWM mode where the compressor is stopped and started with a duty cycle that matches the required cooling capacity. It is necessary to do this when the

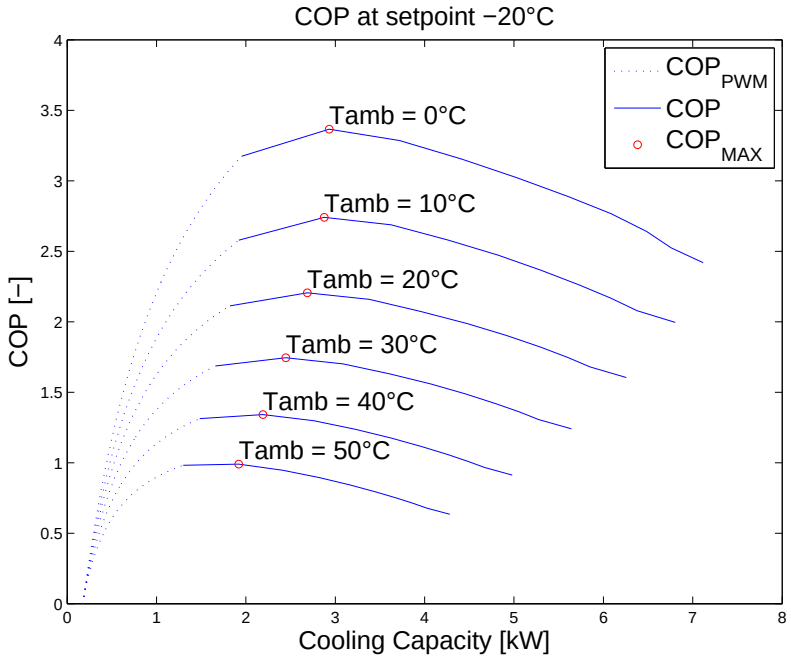

Figure 11: The COP of the refrigeration system at varying ambient temperatures

cooling capacity required to keep the set-point in the container is lower than what is provided by the refrigeration system at the lowest possible compressor speed. The reason for the sharp decline of COP in PWM mode is that the evaporator fan continues running while the compressor is off and therefore the contribution from the fan compared to the cooling capacity is increased as the duty cycle goes towards zero. The expression for the COP in PWM mode is given in Equation (17)

$$COP_{PWM} = \frac{D \cdot Q_{cool-min} - Q_{fan}}{D \cdot P_{cpr-min} + Q_{fan}} \tag{17}$$

where D is the duty cycle, $Q_{cool-min}$ is the cooling capacity at minimum compressor speed, $P_{cpr-min}$ is the consumed compressor power at minimum compressor speed and Q_{fan} is the power consumed by the fan. The ambient temperature has a big impact on both the level and the shape of the COP curve and in order to effectively exploit this, the objective of the MPC must accurately reflect the cost over the length of the prediction horizon. This requires knowledge of the future ambient temperature which is not available and therefore the predictor outlined in section 2.2.1 is used. The predicted ambient temperature is used to select the ap-

propriate COP curve that must be converted to an affine cost that reflects the shape of the COP curve. The COP curve shown here has 9 points because it is generated by simulating the model, described in Section 2.1, to steady state at fixed compressor speeds from 20Hz to 110Hz in increments of 10Hz. For the MPC a set of COP curves is generated at higher resolution for the ambient temperature in order to ensure optimal conditions for the cost optimization.

A linear solver is used and therefore the COP data is converted to a series of linear segments in the form $y = ax + b$ such that they may be used in an epigraph representation of the cost of running the compressor in the objective function. The objective and constraints are listed in Equations (18) to (27):

Objective:

$$P_c(k) + V_{fan}(k) \cdot 195 + T_s(k) \cdot 10^4 \tag{18}$$

Constraints:

$$V_{fan}(k) \cdot Q_{min}(k) <= Q_{cool}(k) <= V_{fan}(k) \cdot Q_{max}(k) \tag{19}$$
$$Q_{cool}(k) \cdot a_1(k) + b_1(k) <= P_c(k) \tag{20}$$
$$Q_{cool}(k) \cdot a_2(k) + b_2(k) <= P_c(k) \tag{21}$$
$$Q_{cool}(k) \cdot a_3(k) + b_3(k) <= P_c(k) \tag{22}$$
$$Q_{cool}(k) \cdot a_4(k) + b_4(k) <= P_c(k) \tag{23}$$
$$V_{fan-min} <= V_{fan}(k) <= 1 \tag{24}$$
$$0 <= T_s(k), \tag{25}$$
$$T_{cargo-min} - T_s(k) <= T_{cargo}(k) <= T_{cargo-max} + T_s(k), \tag{26}$$
$$T_{air}(k) < T_{air-max} + T_s(k) \tag{27}$$

The objective function shown in Equation (18) reflects the power used by the container, expressed by the first and second term where P_c is the power used by the compressor and condenser fan and $V_{fan}(k) \cdot 195$ is the power consumed by the evaporator fans. The constraints given in Equations (20) to (23) are the linear approximation of the convex COP, where the parameters $a_n(k)$ and $b_n(k)$ are derived from the COP curve that matches the predicted ambient temperature at the time of the solution point which results in a cost for the compressor that forms a surface with cooling capacity on one axis and time on the other.

The third term of the objective, the slack variable T_s, is the cost of violating the constraints for cargo and air temperature that is defined in Equation (26) and (27) and it ensures that the controller will keep running and produce solutions in the event that one of the temperature constraints is violated. The cost of violating

the constraint is very high and therefore the controller will prioritize getting back inside the constraints over all other objectives, and this is the desired behavior. The temperature constraints that have been selected for the cargo is $T_{set} \pm 0.25$K and this ensures that the variation in cargo temperature remains small and thereby reducing the risk of damaging the cargo. The model used for the controller lumps the entire cargo into one big volume but in reality the temperature distribution inside the container is non-uniform, see [10], and therefore the air temperature has been constrained to $T_{set}+2$K because this will ensure that the air is cooled and circulated regularly which prevents the buildup of local hot-spots.

3. Results

The objective of the experiments carried out in this work is to identify potential reductions in energy consumption by introducing modern control methods and two different scenarios are investigated at three different ambient temperatures in an attempt to map the power saving potential. The traditional way of controlling the evaporator fan is that it must always be running because the measurement of the cargo temperature is done indirectly through the return air temperature and this measurement becomes invalid when the fans are turned off. But with the cargo estimator it is possible to turn off the fans and use the estimate of the air and cargo temperature instead, which results in a big reduction in consumed energy. It is however interesting to know the fraction of the reduction that comes from cooling storage in the cargo and how much that comes from savings on the fans. Therefore the first scenario use the MPC with the fans forced to be always on and the second scenario allows the MPC to control both the fans and the cooling capacity. The references used in the experiments are simulations using the same linearizing controller as for the MPC, but with a traditional PI controller for generation of the cooling capacity reference. In Figure 12 a section of the simulation results for the reference and the two test scenarios are shown. The two panels on top are the reference simulation, the two panels in the middle are the scenario where the fans are always on and the two panels in the bottom are the scenario where the controller are allowed to turn off the fans. In the reference simulation the fans are running continuously and the controller keeps the cargo and air temperature close to the set-point. The compressor is running in PWM mode and it can be seen that the duty cycle and cooling request is increased at high ambient temperatures to compensate for the higher influx of heat into the cargo hold.

For the scenario where the fans are always on it can be seen that the MPC uses the cargo's thermal inertia allowing the air and cargo temperature to rise to its

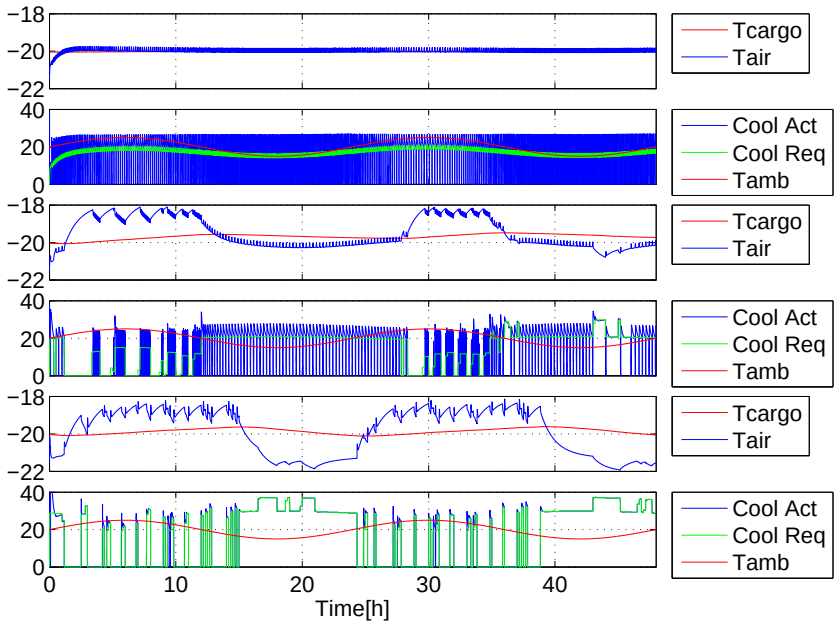

Figure 12: Test results for the reference and the two test scenarios at 20°C ambient temperature.

upper constraint during the period where the ambient temperature is at its highest. The compressor is running in PWM most of the time because there is nothing to gain by running the compressor faster, at a lower efficiency, if it is not possible to turn off the fans for a longer period afterwards.

In the last scenario the fans are turned off when the compressor is not running and the compressor is no longer running PWM but instead at a higher capacity that allows the compressor and fans to be turned off for longer periods, thus saving power. During the periods of high ambient temperature the compressor is only turned on to keep the air temperature below the upper limit while the cargo temperature is slowly increasing and this show that the controller behaves as intended.

The power savings found in the six tests are listed in the following table:

Ambient Temperature	Fans Always ON	Fans ON/OFF
$10 \pm 5°C$	2.53%	21.9%
$20 \pm 5°C$	3.07%	11.1%
$30 \pm 5°C$	2.70%	3.96%

From the results it is obvious that the potential power savings are very dependent on the operating conditions and the reason for this is found in the COP curves on Figure 11 and in the way the refrigeration system was designed. During

normal operation of the container, when the cargo is on its set-point, the system is usually running at a fraction of the cooling capacity that is available, because the system is designed to be able to cool down a hot cargo within reasonable time. But the system is also most efficient when it is running at low capacity because the losses in the system are smaller at low capacity. The COP curve for the compressor alone is monotonically decreasing as the speed increases but when the power from the fans is added the COP curves shown in Figure 11 with a maximum in the lower capacity range emerges. This means that when the amount of cooling needed to keep the set-point in the cargo hold matches the most efficient capacity, the potential energy reduction from being able to turn of the fans is zero. This is reflected by the results that show that the energy savings drops as the ambient temperature increases. When the most efficient mode of operation is running the fans continuously the cargo may still be used as a cooling storage and therefore there will always be something to gain from using this control strategy. In the present experiments a potential saving between 2.5% and 3% is possible with a 10K variation in ambient temperature and with a consumption of 8.9MW for all of the containers on a ship a 2.5% reduction yields 403.7GJ over a 21 day trip which is roughly 10000kg of heavy fuel oil. The six tests presented here show that there is a big difference in potential savings depending on the cooling demand and therefore the further tests should be run to test the entire range of operation of the container, but the large savings will be found where the difference between temperature set-point and ambient temperature is low. Therefore it is expected that it is possible to save a larger percentage of the power for shipments of fruit and vegetables that run at a higher set-point.

4. Conclusion

In this study a model predictive controller that reduced the power consumption of a refrigerated container by turning off the cargo hold fans when they were not needed and using the cargo thermal inertia to store cooling, was presented. Simulation experiments were carried out using a detailed model of the refrigeration system at three different ambient temperatures, with savings in power consumption found to be up to 21%, depending on the set-point. It is expected that larger savings are possible for cargoes that requires a lower set-point. The largest savings were found to be possible only if the controller could control the fans and turn them off when they were not needed. An estimator for cargo temperature, heat capacity, and heat transfer value was developed and used to update the MPC online, thereby enabling optimal exploitation of the available thermal inertia while

keeping the cargo temperature within its constraints. The controller was divided into two layers with the MPC on top providing a cooling power request to a linearizing controller that handled the faster nonlinear dynamics of the refrigeration system. A prediction horizon with varying step sizes led to a reduction in the computational demand from the MPC.

[1] Marinelink, World trade in perishable cargo to grow, 2013. URL: http://www.marinelink.com/news/article/world-trade-in-perishable-cargo-to-grow/328311.aspx.

[2] Container-Handbook, 8.1.2 actual power consumption, 2009. URL: http://www.containerhandbuch.de/chb_e/wild/index.html?/chb_e/wild/wild_08_01_02.html.

[3] R. G. M. van der Sman, G. J. C. Verdijck, Model predictions and control of conditions in a ca-reefer container, in: ISHS Acta Horticulturae 600: VIII International Controlled Atmosphere Research Conference, Agrotechnological Research Institute ATO, P.O. box 17, 6700 AA Wageningen, the Netherlands, 2003, pp. 163–171. URL: http://www.actahort.org/members/showpdf?booknrarnr=600_20.

[4] R. Halvgaard, N. K. Poulsen, H. Madsen, J. B. Jorgensen, Economic model predictive control for building climate control in a smart grid, in: Innovative Smart Grid Technologies (ISGT), 2012 IEEE PES, IEEE, http://orbit.dtu.dk/fedora/objects/orbit:74519/datastreams/file_6543920/content, 2012, pp. 1–6.

[5] Y. Ma, F. Borrelli, Fast stochastic predictive control for building temperature regulation, in: American Control Conference (ACC), 2012, 2012, pp. 3075–3080. doi:doi:10.1109/ACC.2012.6315347.

[6] F. Oldewurtel, A. Parisio, C. Jones, M. Morari, D. Gyalistras, M. Gwerder, V. Stauch, B. Lehmann, K. Wirth, Energy efficient building climate control using stochastic model predictive control and weather predictions, in: American Control Conference (ACC), 2010, 2010, pp. 5100–5105. doi:doi:10.1109/ACC.2010.5530680.

[7] J. E. Braun, Reducing energy costs and peak electrical demand through optimal control of building thermal mass, ASHRAE Transactions (1990) 264–273.

[8] J. E. Braun, R. W. H. Laboratories, Load control using building thermal mass, in: Transactions of the ASME Vol. 125, 2003, pp. 292–301. doi:doi:10.1115/1.1592184.

[9] K. Vinther, H. Rasmussen, R. Izadi-Zamanabadi, J. Stoustrup, A. Alleyne, A learning based precool algorithm for utilization of foodstuff as thermal energy storage, in: Control Applications (CCA), 2013 IEEE International Conference on, 2013, pp. 314–321. doi:doi:10.1109/CCA.2013.6662777.

[10] G. J. C. Verdijck, Model-based product quality control applied to climate controlled processing of agro-material, 2003. URL: http://alexandria.tue.nl/extra2/200310443.pdf.

[11] Wageningen, Agrotechnology & food sciences group, quest-leaflet, 2015. URL: https://www.wageningenur.nl/upload_mm/d/6/b/2b3cd77e-4c34-4a62-95a9-1142267427de_Questleaflet2008.pdf.

[12] J. d. Boogaard, G.J.P.M. van den; Kramer, Quest: Quality and energy in storage and transport of agro-materials, final public report, Wageningen Agrotechnology & Food Sciences Group, (Rapport / AFSG 657), 2006.

[13] A. Jakobsen, B. Rasmussen, M. Skovrup, Development of energy optimal capacity control in refrigeration systems, in: Proceedings of 2000 International Refrigeration Conference, http://docs.lib.purdue.edu/cgi/viewcontent.cgi?article=1498&context=iracc, Purdue University, Indiana, USA, 2000, pp. 329–336.

[14] MCI, Maersk container industry, starcool refrigerated container specifications, 2013. URL: http://www.maerskbox.com/.

[15] Specific heats of common food and foodstuff, 2015. URL: http://www.engineeringtoolbox.com/specific-heat-capacity-food-d_295.html.

[16] S. Engell, Feedback control for optimal process operation, Journal of Process Control 17 (2007) 203 – 219.

[17] L. F. S. Larsen, Model based control of refrigeration systems, 2005. URL: http://www.control.aau.dk/~jakob/phdStudents/lfslThesis.pdf.

[18] B. Rasmussen, A. Musser, A. Alleyne, Model-driven system identification of transcritical vapor compression systems, IEEE Transactions on Control Systems Technology 13 (2005) 444–451.

[19] J. Löfberg, Yalmip is a modelling language for defining and solving advanced optimization problems, 2009. URL: `http://users.isy.liu.se/johanl/yalmip/`.

[20] U. Halldorsson, M. Fikar, H. Unbehauen, Nonlinear predictive control with multirate optimisation step lengths, IEE Proceedings - Control Theory and Applications 152 (2005) 273–285.

[21] BS, British standard/en 12900, refrigerant compressors. rating conditions, tolerances and presentation of manufacturer's performance data, ISBN: 0 580 32694 2, 2005.